

## Local magnetic anisotropy in nanostructured FeCo–C coatings synthesized by green chemistry methods

© E.A. Denisova<sup>1,2</sup>, S.V. Komogortsev<sup>1,2,3</sup>, L.A. Chekanova<sup>1</sup>, D.S. Neznakhir<sup>4</sup>,  
R.S. Iskhakov<sup>1,3</sup>, I.V. Nemtsev<sup>1,2,5</sup>

<sup>1</sup>Kirensky Institute of Physics, Federal Research Center KSC SB, Russian Academy of Sciences  
„Federal Research Center „Krasnoyarsk Science Center of the Siberian Branch of the Russian Academy of Sciences“,  
Krasnoyarsk, Russia

<sup>2</sup>Siberian Federal University,  
Krasnoyarsk, Russia

<sup>3</sup>Reshetnev Siberian State University of Science and Technology,  
Krasnoyarsk, Russia

<sup>4</sup>Ural Federal University after the first President of Russia B.N. Yeltsin,  
Yekaterinburg, Russia

<sup>5</sup>Federal Research Center „Krasnoyarsk Science Center of the Siberian Branch of the Russian Academy of Sciences“,  
Krasnoyarsk, Russia

E-mail: len-den@iph.krasn.ru

Received April 29, 2022

Revised April 29, 2022

Accepted May 12, 2022

Fe–Co alloys attracting interest due to their high magnetic induction and Curie temperature, were synthesized by an eco friendly electroless deposition with carbohydrates as reducing agents. It was shown that  $\text{Fe}_{1-x}\text{Co}_x\text{–C}$  composite coatings retain high induction, while demonstrating an unusual behavior of magnetization at low temperatures. It was found that for each coating measured at different temperatures, there is a correlation between the local magnetic anisotropy constant  $K$  at a given temperature and the correlation radius of the local easy magnetization axis  $R_c$ . The functional type of this correlation is typical for nanoparticles or nanogranules in a composite, which made it possible to estimate the volume and surface magnetic anisotropy constants of metal granules of FeCo–C coatings.

**Keywords:** magnetic anisotropy, FeCo-C coatings, electroless deposition, approach to magnetic saturation law.

DOI: 10.21883/PSS.2022.09.54150.14HH

### 1. Introduction

Films with high saturation induction and nanocomposite coatings based on ferromagnets are the basis for creating ultrasensitive magnetic sensors for various applications, high-density high-speed magnetic recording heads, micro-electronic devices, and radiation protection systems [1–5]. Nanostructured FeCo alloys, characterized by high values of saturation magnetization and magnetic permeability, can be obtained by various methods, including molecular beam epitaxy, magnetron sputtering, electrolytic deposition [6–9]. A promising method is chemical deposition, as it has no restrictions on the size and shape of the surface to be coated. However, the use of traditional reducing agents (hypophosphite or sodium borohydride) leads to significant contamination of the deposited coatings with phosphorus and boron, which leads to deterioration of magnetic characteristics. The use of natural polysaccharides (chitosan, cellulose, arabinogalactan) as reducing agents can become a simple, environmentally friendly and technological method for creating unique nanostructured functional materials [10–14].

Many widely demanded macroscopic magnetic properties of materials are due to the features of their magnetic microstructure, formed by a complex combination of volume-averaged exchange field and magnetic anisotropy field. In nanostructured and composite coatings with a developed surface, the surface anisotropy will make a decisive contribution to the properties of materials. In composites with a high content of the metal phase (exceeding the percolation threshold), the magnetic properties are determined not only by the grain size, but also by the exchange interactions between adjacent grains. When the grain size is less than  $d_{cr} = (A/K)^{1/2}$  (determined by the exchange constant  $A$  and the value of crystallographic anisotropy  $K$ ), the determining role in magnetic hysteresis is played by cooperative phenomena [15]. In the theoretical description, the main parameters of the material here are the correlation length of the local axis of easy magnetization, the local anisotropy constant [16,17]. To independently determine these parameters, an analysis of the approach of magnetization to saturation can be used. This possibility was used by us in the present work.

This paper is devoted to an experimental study of the structure and magnetic properties of FeCo–C coatings

synthesized by chemical deposition using carbohydrates as reducing agents. The main attention is paid to the study of the parameters of local magnetic anisotropy. It will be shown that the discovered correlations between these parameters enable to determine the contributions of the volume and surface magnetic anisotropies to the effective anisotropy of the synthesized coatings.

## 2. Experiment

Coatings  $\text{Fe}_X\text{Co}_{100-X}-\text{C}$  ( $0 < X < 100$ ) were synthesized by chemical deposition based on the reaction of the reduction of metal salts from aqueous solutions. The solution for coating deposition included metal salts (cobalt sulfate  $\text{CoSO}_4 \cdot 7\text{H}_2\text{O}$  and Mohr's salt  $\text{Fe}(\text{NH}_4)_2(\text{SO}_4)_2 \cdot 6\text{H}_2\text{O}$ ); non-toxic sodium citrate ( $\text{Na}_3\text{C}_6\text{H}_5\text{O}_7$ ) was selected as a complexing and at the same time buffering additive; and one of the reducing agents [18,19]. Three types of carbohydrate reducing agents have been used: arabinogalactan (natural polysaccharide  $[(\text{C}_5\text{H}_8\text{O}_4)(\text{C}_6\text{H}_{10}\text{O}_5)_6]_n$ ) — series A; cornstarch ( $(\text{C}_6\text{H}_{10}\text{O}_5)_n$ ) — series B; sucrose ( $\text{C}_{12}\text{H}_{22}\text{O}_{11}$ ) — series C. The deposition was carried out on a copper substrate at a temperature of  $80^\circ\text{C}$ . The pH value was maintained by adding NaOH solution. Coatings with a thickness from 0.6 to  $4\ \mu\text{m}$  were obtained.

The surface morphology and structure of the coatings were studied by electron microscopy (S5500 and TM3000 Hitachi scanning microscopes with an attachment for energy dispersive analysis) and X-ray diffraction (DRON 3). The chemical composition of the samples was determined by the method of energy-dispersive analysis. X-ray photoelectron spectra (XPS) were recorded using a SPECS photoelectron spectrometer (Germany) using an X-ray tube to excite the spectra of monochromatized  $\text{AlK}\alpha$  (1486.6 eV) radiation. The temperature and field dependences of the magnetization were measured on a vibrating magnetometer (Quantum Design). Magnetic characteristics of synthesized materials (saturation magnetization  $M_s$ , exchange interaction constant  $A$ , local anisotropy field value  $H_a$ ) were studied as a function of the Fe, Co, and C content in the alloy.

## 3. Results and discussion

Previously, we showed that varying the composition of the bath for chemical deposition (the Fe:Co ratio, the type of reducing agent) enables to synthesize  $\text{FeCo}-\text{C}$  coatings with a thickness of up to  $4\ \mu\text{m}$  with a uniform distribution of elements, with the ability to control surface morphology and grain size (15–300 nm) [14]. In this article, the chemical deposition method enabled to synthesize both metal films of  $\text{FeCo}(\text{C})$  alloys (Fig. 1, *a*) and  $\text{FeCo}-\text{C}$  composite coatings, which are  $\text{FeCo}$  alloy particles in a polysaccharide matrix (Fig. 1, *b*). According to XPS data, carbon concentration in the  $\text{FeCo}(\text{C})$  alloy does not exceed 1.5 at.% for all series of samples, the rest of the carbon  $\sim 12$  at.% is in the composition of carboxyl and carbonyl groups (the data were

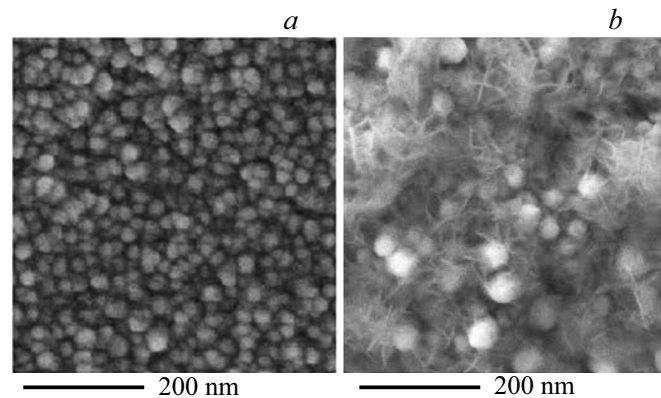


**Figure 1.** SEM-images of  $\text{FeCo}-\text{C}$  coatings obtained with various reducing agents: *a* — arabinogalactan, *b* — starch.

obtained after etching the surface with argon ions, 20 nm of the surface layer was removed). According to the data of energy dispersive analysis in composite films, the carbon content is 11 at.% in metal granules and up to 32 at.% in other areas.

According to X-ray diffraction data for all series of samples,  $\text{Fe}_{1-X}\text{Co}_X-\text{C}$  coatings are characterized by the BCC-structure in a wide range of cobalt concentrations  $X < 96$  (significantly exceeding the equilibrium values for bulk alloys  $X < 75$ ) [20]. At  $X > 96$  the  $\text{FeCo}-\text{C}$  coatings are characterized by an HCP-structure. Thus, it was shown that the non-equilibrium nature of the chemical deposition method enables to change the boundary concentrations of the existence of the BCC-phase of the Fe–Co alloy. It has been established that the maximum value of the saturation magnetization of  $\text{FeCo}-\text{C}$  films is achieved at a cobalt content of 30 at.% and is 205, 235, and 240 emu/g for series A, B, and C, respectively, which enables to attribute these films to the highly inductive class (the magnetization of pure iron is 220 emu/g).

The study of the behavior of magnetization near saturation at low temperatures allows us to draw conclusions — both about local magnetic constants (exchange interaction constant, magnetic anisotropy constant) and about the features of the nanostructure of a ferromagnetic material [21–23]. A series of magnetization curves measured from 5 to 320 K for samples of series A and C demonstrates a change in magnetization approaching to saturation with increasing temperature (Fig. 2 shows a characteristic sequence on the example of a  $\text{Fe}_{30}\text{Co}_{70}\text{film}_{70}-\text{C}$  from series A).

The study of magnetization approaching to saturation is a tool for obtaining quantitative information about the local magnetic anisotropy of a nanocrystalline alloy, which is key in solving problems of controlling the hysteresis properties of films [21–23]. The theoretical basis of these studies is the random magnetic anisotropy model, within which expressions were obtained for the process of magnetization approaching to saturation, which are determined by such parameters as the local anisotropy field  $H_a$  and  $R_c$  — correlation radius of the local axis of easy magnetization.

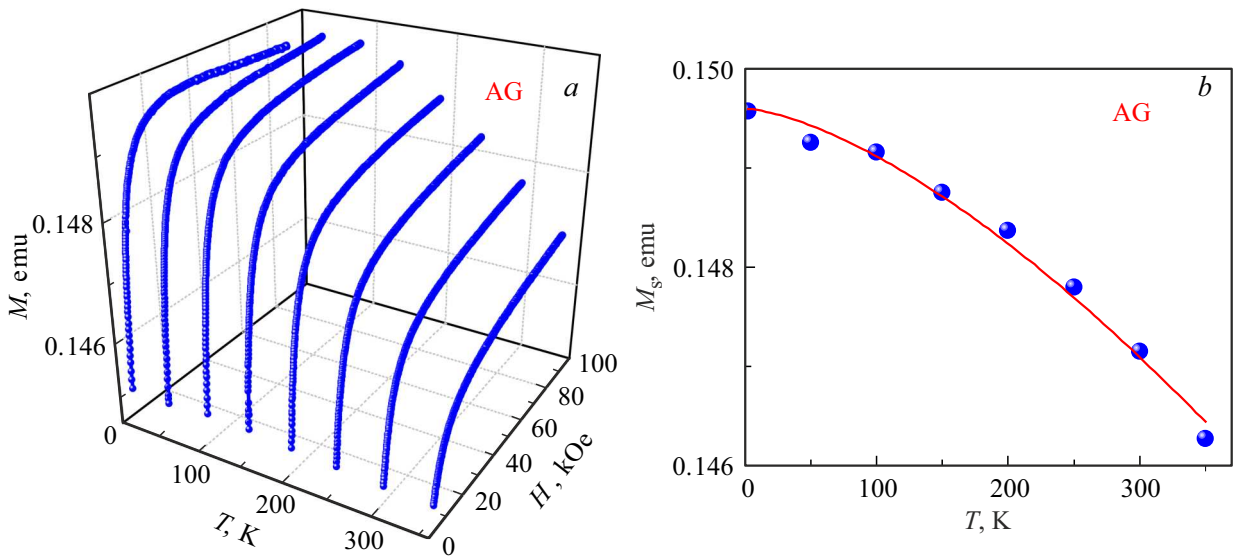


**Figure 2.** Magnetization curves of Fe<sub>30</sub>Co<sub>70</sub>–C alloy films (series A) (a) and the temperature behavior of the saturation magnetization of this film (b), the solid line corresponds to equation (2).

We performed the fitting of magnetization approaching to saturation using the formula derived within the scope of the random magnetic anisotropy model [24]:

$$M(H) = M_s \cdot \left( 1 - \frac{H_a^2}{15H^{1/2}(H^{3/2} + H_R^{3/2})} \right). \quad (1)$$

The parameters  $M_s$  and  $H_a$  characterize the saturation magnetization and the field of local magnetic anisotropy. The parameter  $H_R = 2A/M_s R_c^2$  is the exchange field in the random magnetic anisotropy model (which is the theoretical basis for equation (1) [16]) associated with the constants  $A$ ,  $M_s$  and  $R_c$  — the correlation radius of the local easy magnetization axis. In nanocrystalline alloys, this scale is usually associated with the size of a crystallite [16], in composites with a nanogranule size [22] in amorphous materials, it represents a certain measure of the average order [25]. In the case of our films, which occupy an intermediate position between nanocrystalline alloys and magnetic composites, as we will show below, this size shows some change with temperature. Fitting by formula (1) was performed using the least squares method. The fitting parameters thus obtained corresponded to the minimum of the mean square deviation of the experimental data from (1) in the space of fitting parameters, which indicates their uniqueness and reliability.

The low-temperature behavior of  $M_s$  in films obeys the Bloch  $T^{3/2}$  law (see Fig. 2, b):

$$M_s(T) = M_{s0} \cdot (1 - B \cdot T^{3/2}), \quad (2)$$

which indicates the ferromagnetic nature of the ground state and allowed us to estimate the exchange constant as  $A = \frac{k_B}{8\pi} \left( \frac{M_{s0}}{g\mu_B} \right)^{1/3} \left( \frac{2.612}{B} \right)^{2/3}$  (e.g., see [26]), the values of which for different films are given in Table. Previously,

we showed that the value  $H_a$  of these films, measured at room temperature, increases with increasing Co content and lies within 360–2000 Oe [22]. Films of series B are characterized by the highest value  $H_a$ . For films of series A and C, the values  $H_a$  practically coincide. Based on the field of local anisotropy, one can estimate the value of the local anisotropy constant  $K = H_a M_s / 2$ . In this study, we found a correlation between the parameters  $K$  and  $R_c$  for one film measured at different temperatures (see Fig. 3).

Such a correlation observed for nanoparticles and nanocomposites is explained by the manifestation of the contribution of the surface magnetic anisotropy and enables to separate the contributions of the volume  $K_V$  and surface  $k_S$  anisotropies to the effective local magnetic anisotropy using equation [22]:

$$K = K_V + 6k_S/R_c. \quad (3)$$

This equation successfully describes the observed correlation (see Fig. 3), and the values of  $K_V$  and  $k_S$  of the FeCo–C coatings, obtained as a result of such a description, are presented in the table. It can be seen that the contribution of volume anisotropy increases with an increase in the

Magnetic characteristics of FeCo–C coatings obtained with various reducing agents

Reducing agent	Co, at.%	M, G	A, 10 <sup>-6</sup> erg/cm	$K_V$ , 10 <sup>6</sup> erg/cm <sup>3</sup>	$k_S$ , erg/cm <sup>2</sup>
Arabinogalactan	70	1260	1.98	1.57	0.15
	43	1450	1.74	-0.37	0.24
Starch	18	1340	2	0.55	0.17
	53	1490	1.91	2.78	0.22

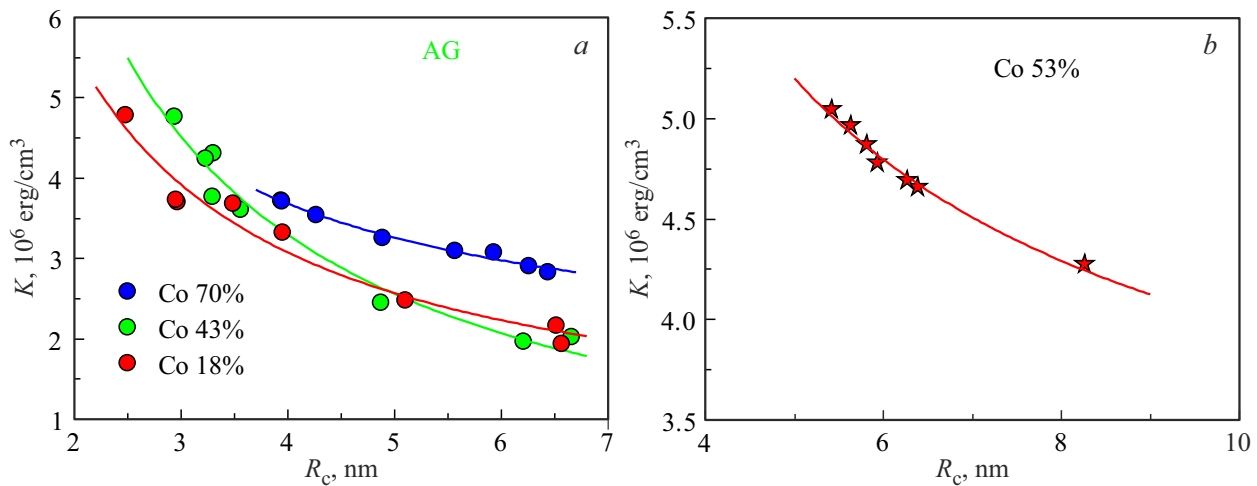


**Figure 3.** Dependence of the anisotropy constant on the value of the correlation radius of the local easy magnetization axis for FeCo–C coatings obtained with various reducing agents: arabinogalactan (a) and starch (b). Solid lines are description of data by equation (3).

cobalt content in the FeCo alloy, which correlates with an increase in the grain size (determined based on the XRD and electron microscopy data) [14].

Volume and surface anisotropy constants show values and change from composition close to those reported in literature [27,28]. This enables to treat with confidence the values  $R_c$  estimated as  $R_c = \sqrt{2A/M_s H_R}$  used in Fig. 3. The change  $R_c$  with temperature up to 2 times, when the temperature changes from 4 to 320 K, looks surprising and means that the local orientation of the easy magnetization axis is hardly directly related to the size of the crystallite. One of the explanations here may be the giant magnetostriction recently discovered in Fe–Co [29] nanocrystalline alloys. The point is that the orientational order of the local easy magnetization axis can be sensitive to the temperature evolution of the structural adjustment of twins and nanophase precipitates, leading to a significant change  $R_c$ .

#### 4. Conclusion

FeCo–C coatings were synthesized using carbohydrates as reducing agents. The effect of the Fe and Co atoms ratio in the alloy on the microstructure and magnetic characteristics of the synthesized samples was determined. The contributions of surface and volume anisotropy to the magnetic anisotropy of FeCo–C composite coatings are estimated.

#### Acknowledgments

The authors are grateful to Yu.L. Mikhlin, V.V. Tkachev, and V.S. Plotnikov for the help in carrying out the measurements.

#### Funding

The study was done with financial support from the Russian Foundation for Basic Research, Government of Krasnoyarsk Territory and the Krasnoyarsk Regional Fund of Science within scientific project No. 20-43-240003.

The authors thank the Krasnoyarsk Regional Research Equipment Sharing Center of the Federal Research Center Krasnoyarsk Science Center of the Siberian Branch of the Russian Academy of Sciences for the provided equipment for measurements.

#### Conflict of interest

The authors declare that they have no conflict of interest.

#### References

- [1] M. Alper, H. Kockar, T. Sahin, O. Karaagac. *IEEE Trans. Magn.* **46**, 1, 390 (2010).
- [2] M. Han, H. Lu, L. Deng. *Appl. Phys. Lett.* **97**, 192507 (2010).
- [3] Y. Cheng, G. Ji, Z. Li, H. Lv, W. Liu, Y. Zhao, J. Cao, Y. Du. *J. Alloys Compd.* **704**, 289 (2017).
- [4] V. Petrov, G. Nikolaichuk, S. Yakovlev, L. Lutsev. *Komponenty i tekhnologii*, **2**, 141 (2008) (in Russian).
- [5] S. Amsarajan, B.R. Jagirdar. *J. Alloys Compd.* **816**, 152632 (2020).
- [6] T. Yanai, K. Shiraishi, Y. Watanabe, T. Ohgai, M. Nakano, K. Suzuki, H. Fukunaga. *J. Appl. Phys.* **117**, 17A925 (2015).
- [7] N.M. Nik Rozlin, A.M. Alfantazi. *Mater. Sci. Eng. A.* **550**, 388 (2012).
- [8] C. Rizal, J. Kolthammer, R.K. Pokharel, B.C. Choi. *J. Appl. Phys.* **113**, 113905 (2013).
- [9] D. Cao, X. Cheng, H. Feng, C. Jin, Z. Zhu, L. Pan, Z. Wang, J. Wang, Q. Liu. *J. Alloys Compd.* **688**, 917 (2016).
- [10] S. Machado, S.L. Pinto, J.P. Grosso, H.P.A. Nouws, J.T. Albergaria, C. Delerue-Matos. *Sci. Total Environ* **445–446**, 1 (2013).  
<https://doi.org/10.1016/j.scitotenv.2012.12.033>.

- [11] B.G. Sukhov, G.P. Aleksandrova, L.A. Grishchenko, L.P. Feoktistova, A.N. Sapozhnikov, O.A. Proydakova, A.V. T'kov, S.A. Medvedeva, B.A. Trofimov. *Zhurn. strukturn. khimii* **48**, 922 (2007) (in Russian).
- [12] V.V. Shulika, A.P. Potapov. *Nanotekhnika* **4**, 66 (2012) (in Russian).
- [13] B. Lu, W. Huang, P. He, C. Yan. *Int. J. Electrochem. Sci.* **7**, 12262 (2012).
- [14] E.A. Denisova, L.A. Chekanova, S.V. Komogortsev, I.V. Nemtsev, R.S. Iskhakov, M.V. Dolgopolova. *J. Supercond. Nov. Magn.* **34**, 2681 (2021).
- [15] G. Herzer. *Acta Mater.* **61**, 718 (2013).
- [16] R.S. Iskhakov, S.V. Komogortsev. *Phys. Met. Metallogr.* **112**, 666 (2011).
- [17] S.V. Komogortsev, E.N. Sheftel. *Materialovedeniye* **10**, 3 (2013) (in Russian).
- [18] E.A. Denisova, L.A. Chekanova, S.V. Komogortsev. *Semiconductors* **54**, 1840 (2020).
- [19] E.A. Denisova, L.A. Chekanova, I.V. Nemtsev, S.V. Komogortsev, N.A. Shepeta. *J. Phys. Conf. Ser.* **1582**, 012077 (2020).
- [20] *Magnetic Properties of Metals d-elements. Alloys and Compound. (Data in Science and Technology)/* Ed. H.P.J. Wijn. Springer (1991). 202 p.
- [21] S.V. Komogortsev, S.V. Semenov, S.N. Varnakov, D.A. Balaev. *FTT* **64**, 25 (2022) (in Russian).
- [22] E.A. Denisova, S.V. Komogortsev, R.S. Iskhakov, L.A. Chekanova, A.D. Balaev, Y.E. Kalinin, A.V. Sitnikov. *JMMM* **440**, 221 (2017).
- [23] S. V Komogortsev, E.A. Denisova, R.S. Iskhakov, A.D. Balaev, L.A. Chekanova, Y.E. Kalinin, A.V. Sitnikov. *J. Appl. Phys.* **113**, 17C105 (2013).
- [24] S.V. Komogortsev, R.S. Iskhakov. *JMMM* **440**, 213 (2017).
- [25] N.V. Ilin, S.V. Komogortsev, G.S. Kraynova, A.V. Davydenko, I.A. Tkachenko, A.G. Kozlov, V.V. Tkachev, V.S. Plotnikov. *JMMM* **541**, 168525 (2022).
- [26] F. Keffer. *Handbuch der Physik. In: Der Phys./Ed. S. Flugge. Springer-Verlag, Berlin (1966).* p. 560.
- [27] R.C. Hall. *J. Appl. Phys.* **30**, 816 (1959).
- [28] L.W. Mc Keehan. *Phys. Rev.* **51**, 136 (1937).
- [29] D. Hunter, W. Osborn, K. Wang, N. Kazantseva, J. Hattrick-Simpers, R. Suchoski, R. Takahashi, M.L. Young, A. Mehta, L.A. Bendersky, S.E. Lofland, M. Wuttig, I. Takeuchi. *Nature Commun.* **2**, 518 (2011).

*Editor T.N. Vasilevskaya*